Unitary Ca^{2+} Current through Mammalian Cardiac and Amphibian Skeletal Muscle Ryanodine Receptor Channels under Near-physiological Ionic Conditions

Claudia Kettlun,[1] Adom González,[2] Eduardo Ríos,[2] and Michael Fill[1]

[1]Department of Physiology, Stritch School of Medicine, Loyola University Chicago, Maywood IL 60153
[2]Department of Molecular Biophysics and Physiology, Rush University School of Medicine, Chicago IL 60612

ABSTRACT Ryanodine receptor (RyR) channels from mammalian cardiac and amphibian skeletal muscle were incorporated into planar lipid bilayers. Unitary Ca^{2+} currents in the SR lumen-to-cytosol direction were recorded at 0 mV in the presence of caffeine (to minimize gating fluctuations). Currents measured with 20 mM lumenal Ca^{2+} as exclusive charge carrier were 4.00 and 4.07 pA, respectively, and not significantly different. Currents recorded at 1–30 mM lumenal Ca^{2+} concentrations were attenuated by physiological $[K^+]$ (150 mM) and $[Mg^{2+}]$ (1 mM), in the same proportion (~55%) in mammalian and amphibian channels. Two amplitudes, differing by ~35%, were found in amphibian channel studies, probably corresponding to α and β RyR isoforms. In physiological $[Mg^{2+}]$, $[K^+]$, and lumenal $[Ca^{2+}]$ (1 mM), the Ca^{2+} current was just less than 0.5 pA. Comparison of this value with the Ca^{2+} flux underlying Ca^{2+} sparks suggests that sparks in mammalian cardiac and amphibian skeletal muscles are generated by opening of multiple RyR channels. Further, symmetric high concentrations of Mg^{2+} substantially reduced the current carried by 10 mM Ca^{2+} (~40% at 10 mM Mg^{2+}), suggesting that high Mg^{2+} may make sparks smaller by both inhibiting RyR gating and reducing unitary current.

KEY WORDS: ryanodine receptor • Ca^{2+} release • sarcoplasmic reticulum

INTRODUCTION

The contractile proteins in skeletal muscle are activated by a sudden increase in cytosolic Ca^{2+} concentration. The cytosolic Ca^{2+} level is largely determined by the balance of Ca^{2+} uptake and release by the SR. Calcium is released from the SR through a specialized Ca^{2+} channel, the RyR. Functional, biochemical, and electron microscopic studies have recently called attention to striking differences between these channels in different taxonomic classes. Mammalian skeletal muscle predominantly contains the RyR1 channel isoform (McPherson and Campbell, 1993; Coronado et al., 1994; Ogawa, 1994). The RyR3 channel isoform is also expressed in mammalian striated muscles, but at relatively low levels (Sutko et al., 1991; Tarroni et al., 1997; Froemming et al., 2000). Amphibian skeletal muscle contains nearly equal amounts of the α- and β-RyR isoforms, which are homologues of mammalian RyR1 and RyR3, respectively (Lai et al., 1992; Airey et al., 1993; Oyamada et al., 1994; Sutko and Airey, 1996).

In skeletal muscle, some RyR channels are physically associated with dihydropyridine receptors (DHPRs) in the transverse (T-) tubule membrane. The DHPRs sense the T-tubule membrane depolarization and transmit this information to the RyR channel. This signal triggers the DHPR-linked RyR channels to open and release Ca^{2+} from the SR. At least in amphibians, it is proposed that this depolarization-induced Ca^{2+} release (DICR) activates nearby DHPR-free RyR channels through the Ca^{2+}-induced Ca^{2+} release (CICR) mechanism. It is not known whether or not this duality of mechanisms translates to the existence of two additive components of Ca^{2+} release (as proposed in a model of Ríos and Pizarro, 1991). Whether and how different Ca^{2+} release activation mechanisms may correspond to the different types of RyR channels present is also uncertain.

A new dimension to this duality was recently added by Felder and Franzini-Armstrong (2002), who presented evidence that β isoforms occur in parajunctional arrays, while α-RyR1 isoforms constitute the T-tubule–facing, junctional arrays. It would be reasonable to expect different functional properties for channels that are not just molecular variants but are also arranged differentially in the terminal cisternae of the SR.

Spatially and temporally discrete Ca^{2+} release events called "Ca^{2+} sparks" were first observed in mammalian cardiac muscle cells (Cheng et al., 1993). Analogous

Address correspondence to Michael Fill, Department of Physiology, Loyola University Chicago. 2160 S. First Ave., Maywood, IL 60153. Fax: (708) 216-5158; email: mfill@lumc.edu

Abbreviations used in this paper: CICR, Ca^{2+}-induced Ca^{2+} release; DHPR, dihydropyridine receptor; DICR, depolarization-induced Ca^{2+} release.

J. Gen. Physiol. © The Rockefeller University Press • 0022-1295/2003/10/407/11 $8.00
Volume 122 October 2003 407–417
http://www.jgp.org/cgi/doi/10.1085/jgp.200308843

events occur in amphibian skeletal muscle (Tsugorka et al., 1995; Klein et al., 1996; Kirsch et al., 2001). Additionally, spark-like events have also been recorded in mammalian skeletal muscle (Conklin et al., 1999; Kirsch et al., 2001; Zhou et al., 2003). The number of RyR channels that underlie an individual spark is still debated (e.g., Ríos and Brum, 2002; Schneider and Ward, 2002). Part of the debate stems from uncertainty concerning the amplitude of Ca^{2+} current carried by a single RyR channel in the cell. Although ingenious indirect estimates of unitary RyR Ca^{2+} current in situ have been produced (see Wang et al., 2001), its direct measurement requires that the channel be isolated from the cell and reconstituted into an artificial lipid bilayer (Smith et al., 1985; Fill and Coronado, 1988). However, most RyR channel studies in bilayers have been done under conditions designed to optimize the signal-to-noise characteristics, conditions that typically include high [Ca^{2+}] and/or the use of nonphysiological concentrations of other ions.

Defining the attributes of the Ca^{2+} release channels in near-physiological conditions requires more than simply adjusting the Ca^{2+} concentrations. Indeed, the RyR channels are poorly selective Ca^{2+} channels, which do not discriminate well between divalent cations and discriminate only poorly between divalent and monovalent cations. Thus, several cations present in the cell (i.e., Ca^{2+}, Mg^{2+}, and K^+) can permeate through an open RyR channel. This is important because the Mg^{2+} and K^+ concentrations in the cytosol are large and the presence of these ions is known to reduce the unitary Ca^{2+} current.

Earlier work of our laboratories (Mejía-Alvarez et al., 1999) defined the unitary Ca^{2+} currents carried by single RyR channels isolated from mammalian heart in quasiphysiological salt solutions (150 mM Cs^+, 1 mM Mg^{2+} with variable lumenal Ca^{2+} levels). The measured current was 0.35 pA when the lumenal Ca^{2+} concentration ($[Ca^{2+}]_L$) was 2 mM in the presence of 150 mM Cs^+ symmetrical with no Mg^{2+} present. One shortcoming of these original measurements was the possibility that rapid closures and the limited bandwidth of bilayer recordings could have led to an underestimate of the current. Another was the presence of Cs^+ as permeable monovalent cation. This may be important because this ion is substantially less permeant than K^+ ($pCs^+/pK^+ = 0.61$; Williams et al., 2001). We now provide new measurements in an attempt to correct these limitations. A high caffeine concentration was used to prolong the open state (i.e., to reduce the potential impact of rapid closures) and the permeable monovalent cation was K^+ (not Cs^+). Additionally, we extended the measurements to include frog skeletal muscle channels, so that the results can also be applied to interpretation of sparks in amphibian skeletal muscle. Finally, in light of the interest in using Mg^{2+} as a modulator of Ca^{2+} spark frequency and morphology (González et al., 2000; Lamb, 2000; Lamb, 2002), we performed measurements of current in the presence of variable Mg^{2+} concentrations.

MATERIALS AND METHODS

Heavy SR microsomes were isolated from the leg muscles of the frog *Rana pipiens* or pig cardiac muscle using previously described methods (Tate et al., 1985). Single SR Ca^{2+} release channels were reconstituted by fusing heavy SR microsomes into artificial planar lipid bilayers formed across a 150-μm diameter hole in the wall of a Delrin cup. The cup was placed in a plastic block so that the bilayer separated two pools (cis and trans). Each pool was filled with a solution containing 20 mM HEPES-TRIS (pH 7.4) and 10 μM added free Ca^{2+}. All other salts and pharmacological agents were added to this solution. All experiments were done in the presence of 5 or 10 mM symmetrical caffeine for cardiac or skeletal ryanodine receptors, respectively. In this study, TRIS was considered an impermeable cation. Although large cations can permeate through the RyR channel, to our knowledge there is no report of TRIS permeation through a RyR channel. Even if TRIS were permeable, the relatively low concentration used here makes it unlikely to substantially alter the interpretation of our results. In the frog studies, two current amplitudes were observed, believed to belong to two classes of channels. Unless specified otherwise, frog data and analysis were done on currents believed to correspond to the larger conductance class.

Bilayers were formed using a lipid mixture of phosphatydylethanolamine and phosphatydylcholine (7:3, 50 mg/ml decane; Avanti Polar Lipids, Inc.). Heavy SR microsomes were added to the cis pool. The trans pool was held at virtual ground. Small aliquots (2 μl) of a 4 M $CsCH_3SO_3$ solution were squirted (providing a brief period of high $CsCH_3SO_3$ concentration) at the cis side of the bilayer to facilitate RyR incorporation. In our experience, the use of $CsCH_3SO_3$ (compared with other salts) provided the best rate of single RyR channel incorporation. The total $CsCH_3SO_3$ added was always well below 1 mM. An equal amount of $CsCH_3SO_3$ was added to the trans chamber. Recording electrodes were carefully balanced and the transmembrane potential was held at 0 mV (unless otherwise stated). The polarity of RyR insertion was such that the channel's cytosolic side was always in the cis pool (Fill et al., 1990). The channels were positively identified by their sensitivity to ryanodine (unpublished data) and caffeine.

The Debye-Huckel equation was used to calculate the Ca^{2+} activity coefficient (γ_{Ca}) in the different experimental solutions used in this study (control, 1 mM $MgCl_2$, 150 mM KCl, 1 mM $MgCl_2$ and 150 mM KCl; also see Fig. 7 A). The hydrated ionic radii of Mg^{2+}, Ca^{2+}, K^+, and Cl^- were assumed to be 0.8, 0.6, 0.3, and 0.3 nm, respectively. The ionic strength in each experimental situation was determined with 1 to 5 mM $CaCl_2$ present. The estimated range of γ_{Ca} was 0.665–0.564 in the control and Mg-only studies. The range of γ_{Ca} was substantially less (i.e., 0.350 to 0.341) in the KCl and KCl-Mg solutions. Thus, the γ_{Ca} should be considered when interpreting and/or extrapolating the Ca^{2+} concentration data presented here.

Unitary currents were recorded using a conventional patch clamp amplifier (Axopatch 200B; Axon Instruments, Inc.). The current signal was digitized at 4 kHz with a 16-bit AD/DA converter (Digidata 1200; Axon Instruments, Inc.) and Bessel-filtered at 1 kHz. Unitary current amplitude measurements were made by either measuring the difference between mean open/closed currents from individual adjacent long open/closed

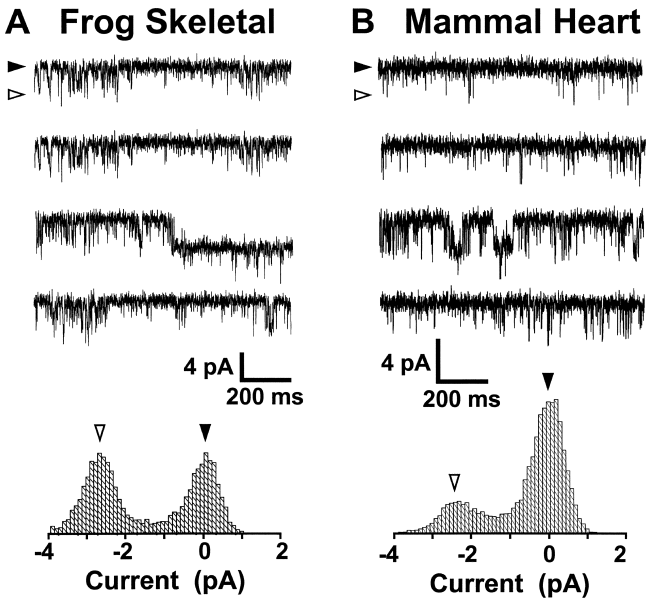

FIGURE 1. Unitary Ca^{2+} current of amphibian (A) or mammalian (B) RyR channels in the absence of competing ions. In this and the following figures currents were recorded at 0 mV in the presence of caffeine (10 or 5 mM, see MATERIALS AND METHODS), and filtered at 1 kHz. Open events are shown as downward current deflections. Records in the figure were at 5 mM $[Ca^{2+}]_L$. The open state is marked by a filled arrowhead. The closed state is marked by an open arrowhead. Corresponding all-points histograms reveal channel currents of <3 pA.

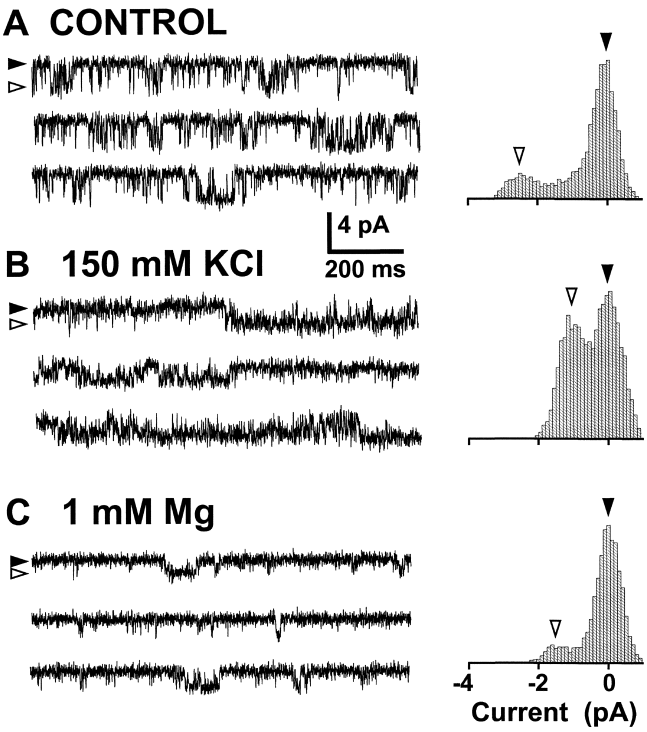

FIGURE 2. Mammalian RyR2 channel current is attenuated by physiological levels of K^+ or Mg^{2+}. $[Ca^{2+}]_L$ was 2 mM. All data were collected from the same single channel. (A) Representative control recordings and all-points histogram. (B) Current after symmetrical addition of 150 mM KCl. (C) Current after solutions were changed to contain symmetrical 1 mM Mg^{2+}.

events and/or by the difference between means of two Gaussian curves fit to all-points histograms. Data acquisition, unitary current measurement, statistical analysis, and data processing were performed using commercially available software packages (pClamp V6.0, Axon Instruments, Inc.; Origin, Microcal). The all-point histograms were generated from 1 to 4 min of recording using pClamp. The ordinates (unpublished data) represent the number of points. Abscissas in the histograms were shifted so that the closed current peak was at 0 pA. Data were plotted as mean ± SEM. Paired comparisons were statistically evaluated using a two-tailed Student's *t* test (Rosner, 1982).

Model Simulations and Fitting

The four-barrier permeation model of Tinker et al. (1992) was used to calculate current at different ion concentrations, and implemented in a program kindly provided by Drs. Andrew Tinker (University College, London) and Alan L. Williams (Imperial College, London). The model is identical to that applied by Tinker et al. (1992). It describes permeation as a series of transitions obeying Eyring rate theory through a free energy profile consisting of 4 peaks and 3 wells. The electrical distances of the wells from the cytosolic edge were 0.1, 0.5 and 0.9. Predictions were done assuming a holding potential of 0 mV. The ion concentration of Ca^{2+}, Mg^{2+}, K^+ were as stated in the text. The heights (in RT units) of the voltage- and concentration-independent local extremes of energy for Ca^{2+} were 3.00, 3.00, 3.00, 3.00, −2.35, −9.50, and −2.35 for peaks 1 through 4, and wells 1 through 3, respectively. The corresponding parameters for Mg^{2+} were 3.00, 3.00, 3.00, 3.00, −2.35, −9.80, and −2.35. For K^+ they were 5.50, 5.50, 5.50, 5.50, −2.35, −3.25, and −2.35. Note that the energy profile for Mg^{2+} has a central well 0.3 RT deeper than that for Ca^{2+}.

Additional fitting was performed with an extension of the Poisson-Nernst-Plank model of electrodiffusion (Chen et al., 1999, 2003). In this case each ion's diffusion is driven by the gradient of a chemical potential with a concentration term, an electrical term, and an excess potential (μ^*) describing chemical interactions with the pore wall (Chen et al., 1999). The adjustable parameters include a diffusion coefficient and excess potential for each ion, as well as parameters of a simple geometry and charge profile for the channel. Geometry, charge profile, and parameters of monovalent ions are in Table 3 of Chen et al. (1999). The current versus $[Ca^{2+}]$ data were well fit with $D_{Ca} = 8 \times 10^{-8} cm^2/s$, $\mu^* = -91$ mV, $D_{Mg} = 5 \times 10^{-8}$ cm^2/s, $\mu^* = -53$ mV.

For visualization purposes, some datasets were fit by a single rectangular hyperbolic function of lumenal Ca concentration using the following equation:

$$I_{OBS} = i_{MAX} \times \{(B \times [Ca]_L)/(1 + (B \times [Ca]_L))\}. \quad (1)$$

Here, i_{OBS} is the experimentally observed unitary current, i_{MAX} is the maximum unitary current measured at high $[Ca]_L$ levels and B is the inverse concentration at half-maximal current.

RESULTS

The goal here was to measure unitary RyR channel currents carried by Ca^{2+} in the trans to cis (i.e., lumen to

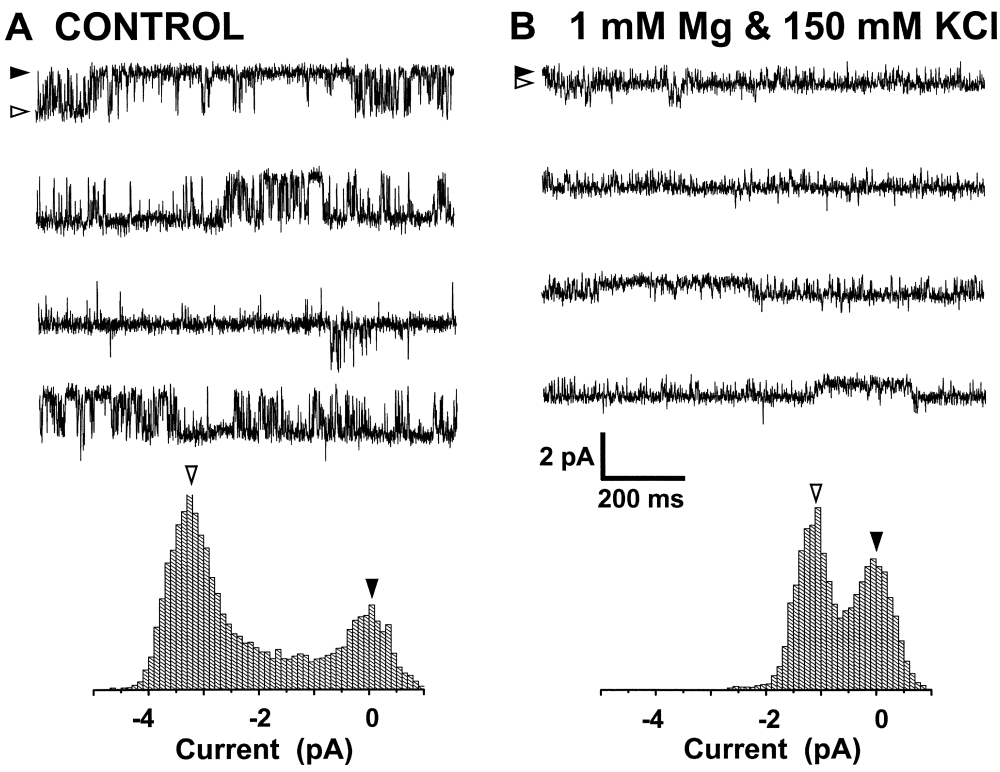

FIGURE 3. Amphibian skeletal muscle RyR channel current is attenuated by physiological levels of K^+ or Mg^{2+}. $[Ca^{2+}]_L$ was 4 mM. (A) Representative recording and corresponding all-points histogram. (B) Current after symmetrical addition of 150 mM KCl and 1 mM Mg^{2+}.

cytosol) direction. These measurements were done at 0 mV in the presence of a trans-to-cis Ca^{2+} gradient. Other permeant cations (i.e., K^+ and Mg^{2+}) were added symmetrically (i.e., to both sides of the bilayer) in some experiments. Net currents carried by these ions did not contribute to the unitary current at 0 mV because of the absence of driving force. To reduce open channel current measurement errors due to fast gating fluctuations, recordings were performed in the presence of symmetrical 10 or 5 mM caffeine to induce longer open events. In the first section below, the impact of 150 mM K^+ and 1 mM Mg^{2+} on unitary Ca^{2+} current is explored. The second section presents a series of measurements at different $[Ca^{2+}]_L$, including those believed to apply physiologically.

Unitary Currents in the Presence of Caffeine

In the presence of 10 mM caffeine, a substantial increase in the open probability (Po) of the RyR channel was noted upon addition of KCl (as reported by Meissner et al., 1997). The effect was greater in the cardiac than in the skeletal channel. The observed increase in Po made it difficult to measure current amplitude because closures were relatively infrequent. To circumvent this problem, cardiac channel studies were done at a lower caffeine concentration (5 mM). The current amplitude of the channel was identical at both caffeine concentrations. All data shown represent results in the presence of 5 mM caffeine (for cardiac preparations) or 10 mM caffeine (for skeletal muscle channels).

Representative records of a frog skeletal and a mammalian heart RyR channel are shown in Fig. 1, A and B. Single-channel activity was measured in the presence of 5 mM $[Ca^{2+}]_L$ in the standard recording solutions (i.e., 20 mM Tris-HEPES, pH 7.4). The free Ca^{2+} concentration on the cytoplasmic side of the channel was ~10 μM. No competing ions (K^+ or Mg^{2+}) were present. Single channel openings (current in trans to cis direction) are shown as downward deflections from the zero current level (filled arrowhead). The corresponding total amplitude (i.e., all-points) histograms are shown at the bottom. The unitary current was <3 pA in both cases.

The effect of other permeant ions on the unitary Ca^{2+} current carried by a mammalian cardiac RyR channel (RyR2) is shown in Fig. 2. In the absence of other permeant ions (Fig. 2 A), Ca^{2+} current at 0 mV was slightly larger than 2 pA when $[Ca^{2+}]_L$ was 2 mM. Addition of 150 mM KCl (Fig. 2 B) or 1 mM Mg^{2+} (Fig. 2 C) symmetrically (i.e., to both sides of the channel) reduced the current to <2 pA. These data were collected from the same RyR2 channel.

The influence of K^+ and Mg^{2+} on the unitary Ca^{2+} current of a frog RyR channel is demonstrated in Fig. 3. The Ca^{2+} current at 0 mV with 4 mM $[Ca^{2+}]_L$ in the absence of other permeable ions was slightly larger than 3 pA (Fig. 3 A). The addition of 150 mM KCl and 1 mM Mg^{2+} (Fig. 3 B) to both chambers reduced it to nearly 1 pA. In summary, the presence of physiologically relevant concentrations of K^+ and Mg^{2+} reduces substan-

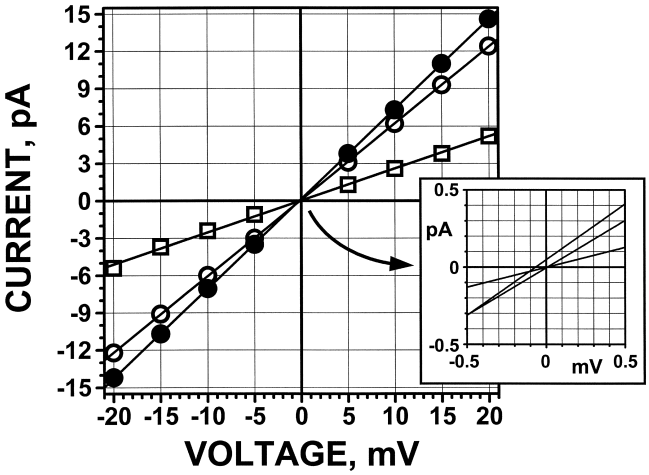

FIGURE 4. Current-voltage relationships of a RyR channel of amphibian skeletal muscle in the presence of different KCl concentrations. Squares, 50 mM KCl; open circles, 100 mM; filled circles, 200 mM. All data were collected on the same channel while salt concentration was increased by serial symmetrical additions. At each salt concentration data were well fit by a straight line. The slope conductances were 258, 613, and 721 pS for the 50, 100, and 200 mM datasets, respectively. Current reversed very close to 0 mV in all cases (inset).

tially the unitary Ca^{2+} current of the mammalian and amphibian RyR channels.

The high K^+ and Mg^{2+} permeability of the RyR channels is well documented (Smith et al., 1988; Lindsay et al., 1991; Tinker and Williams, 1992). The decrease in unitary Ca^{2+} current in the presence of these ions has been interpreted as a consequence of competition by K^+ and Mg^{2+} for occupancy of sites in the RyR pore (Mejía-Alvarez et al., 1999). This interpretation is also buttressed by simulations using a barrier model of permeation (shown below).

Accuracy of Solution Changes and Electrode Balancing

These studies involve measurement of relatively small unitary currents before and after addition of relatively large salt concentrations (K^+ and/or Mg^{2+}) to both sides of the bilayer. Relatively small errors in the salt addition and/or electrode balancing can affect the unitary current measurement. To evaluate these potential sources of error, current-voltage relationships of single amphibian RyR channels were measured after a series of symmetric KCl additions (50, 100, and 200 mM; Fig. 4). There was no Mg^{2+} present, the free Ca^{2+} concentration on each side of the channel was 10 μM, and caffeine was added symmetrically at 10 mM. Averaged results from six channels are represented in Fig. 4. All three current-voltage plots were Ohmic and reversed near 0 mV. The unitary current at 0 mV varied within a relatively small range (0.05 pA; see Fig. 4 inset). These data indicate that large symmetric salt additions could be made without introducing substantial error in the current measurements.

Frog Unitary Currents Display Two Amplitudes

In the frog studies, multiple current levels were observed frequently, suggesting that multiple channels incorporated into the bilayers. In these records, different current amplitudes (or conductances) were frequently observed in the experimental conditions tested (43% of the cases). A sample multilevel record with different current amplitudes is shown in Fig. 5 (top). The corresponding all-points histogram (bottom) has peaks corresponding to the current amplitudes occurring individually, and both occurring simultaneously. The two individual amplitudes, defined in the histogram as the difference between the individual peaks and the baseline (see horizontal bars with numbers in panel B), differed by ~35%. Both classes of openings were sensitive to ryanodine.

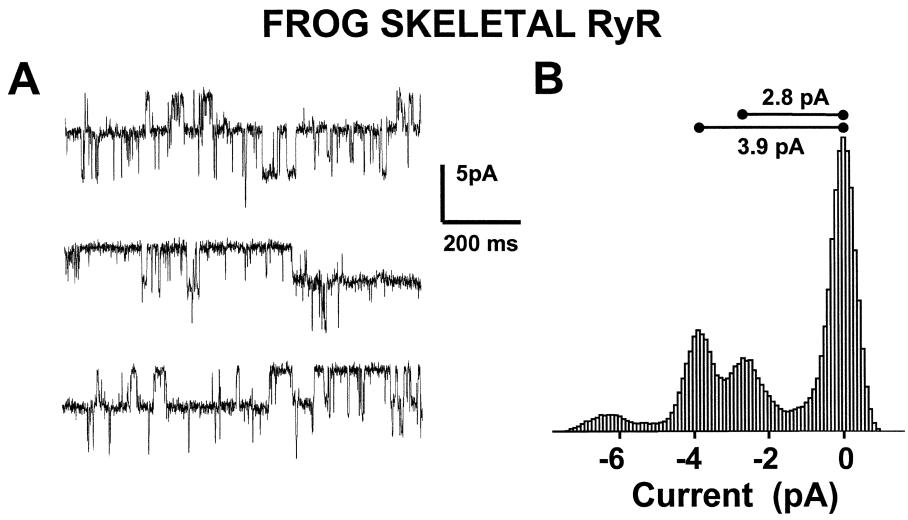

FIGURE 5. Different current amplitudes suggest the presence of two classes of channels. (A) Example multilevel recording acquired under control conditions (no competing ions). $[Ca^{2+}]_L$ was 20 mM. Cytosolic $[Ca^{2+}]$ was 10 μM. (B) Corresponding all points histogram. Note peaks at two different individual amplitudes and their sum.

The characteristics of these events are examined further in Fig. 6. In panel A, histograms are presented of the individual amplitudes (determined as in Fig. 5) exclusively in bilayers that had two different amplitudes simultaneously. The individual distributions were well fitted by single Gaussian functions (fits depicted by continuous curves) and the average currents were significantly different ($P < 0.001$). The study in Fig. 6 B helps test whether these two amplitudes correspond to different channels. The dashed line represents the distribution of the larger current amplitudes in part A. The histogram (crosshatched bars) represents current amplitudes found in bilayers with only one clearly distinguishable level (and those with multiple but equal levels). The line is a fit using the sum of two Gaussian functions. The good fit suggests that there are two groups of individually appearing channels with unitary currents like those observed in the multilevel recordings. Hence, it can be reasonably concluded that the two amplitudes correspond to different channels, which insert individually, and sometimes together. The roughly similar number of bilayers with two different currents and two equal (high) currents is consistent with the possibility that the channels insert independently with roughly equal probability.

The α- and β-RyR channel isoforms are present in frog skeletal muscle in roughly equal amounts. Thus, it is possible that the two current amplitudes observed above correspond to these different RyR isoforms. There is no previously published evidence that these two isoforms have different conductance. In the mammal, however, Murayama et al. (1999) reported a significantly greater (~16%) monovalent cation conductance of RyR3 over RyR1. Clearly, more experimentation is necessary before a solid interpretation concerning the two observed conductances here can be made. The frog RyR channel measurements that follow were done on channels in the larger conductance class.

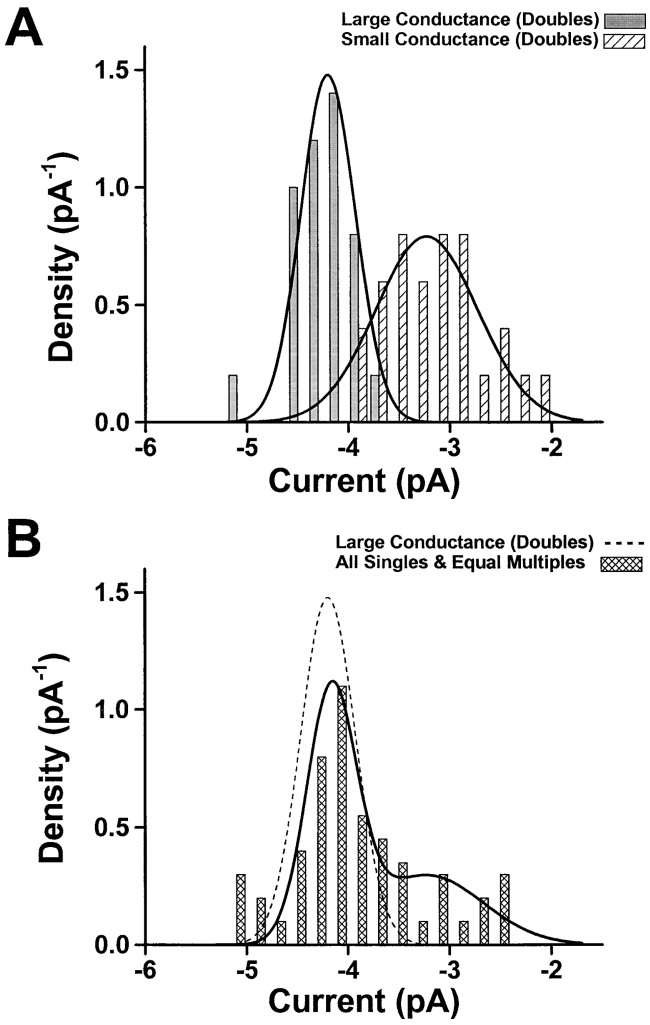

FIGURE 6. Distribution of current amplitudes in frog skeletal channels. The curve fits are either one or the sum of two Gaussian functions of current I (i.e., $a_1 \exp(-(I - \mu_1)^2/2\sigma_1^2)$. (A) Average values from bilayer experiments that featured two different current amplitudes, as illustrated in Fig. 5. The two histograms plot separately high (filled bars) and low (hatched bars) amplitudes at 20 mM $[Ca^{2+}]_L$. The fit parameters are $\mu_1 = -4.19$ pA, $\sigma_1 = 0.539$, $\mu_2 = -3.22$ pA and $\sigma_2 = 1.01$. (B). The dotted line represents the Gaussian fit of the high current amplitudes presented in part A. The crosshatched bars represent amplitudes in bilayer experiments that had one level, or multiple levels at equal intervals. The solid curve represents a constrained fit with the sum of two Gaussians: $a_1 = 0.71$, $\mu_1 = -4.14$ pA, $\sigma_1 = 0.65$, $a_2 = 0.41$, $\mu_2 = -3.22$ pA and $\sigma_2 = 1.10$.

Lumenal Ca^{2+} Concentration Dependence of Unitary Current

The Ca^{2+} current carried by single mammalian or amphibian RyR channels was defined in four different experimental conditions over a wide range of $[Ca^{2+}]_L$. These conditions are illustrated in Fig. 7 A. In the first experimental condition (control; filled triangles), the only permeable ion present was Ca^{2+}. In the second condition (open circles), 1 mM Mg^{2+} was added to each side of the channel so that there were two permeable cations present (Ca^{2+} and Mg^{2+}). In the third condition (filled circles), 150 mM K^+ was added symmetrically instead of the Mg^{2+} and the result was that there were two permeable cations present (Ca^{2+} and K^+). In the final case (half-filled circles), 1 mM Mg^{2+} and 150 mM K^+ were added symmetrically.

Several channels were studied in each condition. The summary data (means ± SEM; n = 5–22 channels per point) are plotted as a function of $[Ca^{2+}]_L$ in Fig. 7 B for the mammalian RyR channel and in Fig. 7 C for the amphibian RyR channel. The lowest $[Ca^{2+}]_L$ at which clearly resolved unitary currents could be measured was 1 mM. In every condition, unitary current at 0 mV increased less than proportionally with $[Ca^{2+}]_L$, tending toward saturation at high $[Ca^{2+}]_L$ levels. Each set of data points was fit with a single rectangular hyperbolic

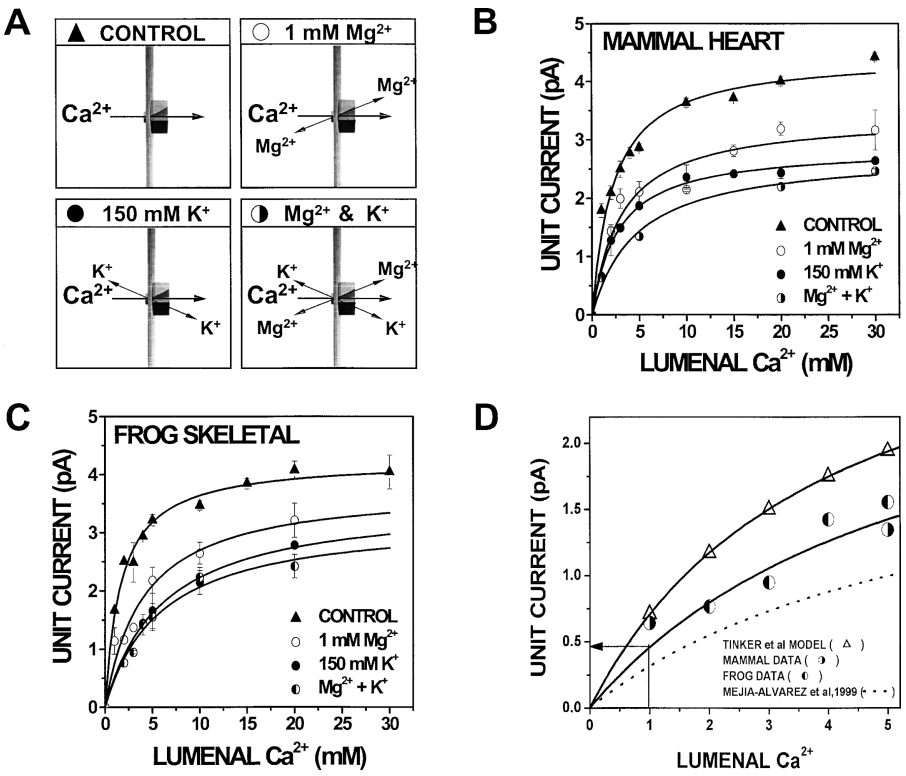

FIGURE 7. Unitary Ca^{2+} current of amphibian and mammalian RyR channels in the presence of competing ions. (A) Schematic representation of the four different salt conditions examined. Filled triangle, control (Ca^{2+} in the absence of other permeant ions). Open circle, symmetric 1 mM Mg^{2+}. Filled circle, symmetric 150 mM K^+. Half-open circle, symmetric 1 mM Mg^{2+} and 150 mM K^+. (B) Unitary Ca^{2+} current carried by the mammalian RyR2 channel in each condition, plotted vs. $[Ca^{2+}]_L$. The curves are fits obtained using equation 1 with parameters B and i_{MAX}. The B values are 0.45, 0.33, 0.37 and 0.32 mM^{-1} for the control, Mg-only, K-only, and Mg-K datasets, respectively. The corresponding i_{MAX} values are 4.44, 3.42, 2.87 and 2.76 pA. (C) Unitary Ca^{2+} current (at 0 mV) carried by the amphibian skeletal muscle RyR in each test condition, plotted versus $[Ca^{2+}]_L$. Again, the curves were fit using Eq. 1. The B values are 0.51, 0.24, 0.17, and 0.17 for the control, Mg-only, K-only, and Mg-K datasets, respectively. The corresponding i_{MAX} values are 4.25, 3.79, 3.56, and 3.26 pA. (D) The mammalian and amphibian Mg^{2+} and KCl datasets replotted on an expanded scale. Open triangles, currents calculated with the 4-barrier model (see methods) assuming symmetric 1 mM Mg^{2+} and 150 mM K^+. The dotted line represents the published data of Mejía-Alvarez et al. (1999) collected in symmetrical 150 mM $CsCH_3SO_3$.

function passing through the origin. For both mammalian and amphibian channels, the presence of competing ions attenuated unitary current at all $[Ca^{2+}]_L$ tested. The attenuation induced by the presence of 1 mM Mg^{2+} was less than that induced by 150 mM K^+. Current reduction was greatest when both K^+ and Mg^{2+} were present.

The concentration of Ca^{2+} inside the SR is thought to be close to 1 mM in cardiac muscle and 1–5 mM in skeletal muscle (Hasselbach and Oetliker, 1983; Volpe and Simon, 1991; Inesi, 1994; Chen et al., 1996; Shannon and Bers, 1997). The membrane potential across the SR in situ is thought to be at or very close to 0 mV (Somlyo et al., 1981; Gilbert and Meissner, 1983; Best and Abramcheck, 1985; Tang et al., 1989). To better estimate unit Ca^{2+} current at such low Ca^{2+} levels, a small segment of the datasets shown in Fig. 7, B and C, are expanded and superimposed in Fig. 7 D. The mammalian and amphibian data nearly overlap (half-filled circles). These data indicate that the unit Ca^{2+} current carried by the mammalian or amphibian RyR channels in the presence of physiological Mg^{2+} and K^+ concentrations is slightly less than 0.5 pA (red arrow in Fig. 7 D). The dashed line represents a previously published dataset (Mejía-Alvarez et al., 1999) collected on RyR2 channels with 150 mM symmetrical Cs^+, no Mg^{2+}, and no caffeine.

In Fig. 7 D, the experimental results are compared with predictions of the well-known 4-barrier Eyring rate model of Tinker et al. (1992), applied with the parameters outlined in the methods section. The open triangles represent values of current calculated at the Ca^{2+} concentrations in the abscissa, with Mg^{2+} and K^+ included in the model at the levels used here. The model predicts currents generally greater than that experimentally observed, but reproduces well their tendency with increasing $[Ca^{2+}]$, as well as the changes observed in high $[Mg^{2+}]$.

Unitary Currents in the Presence of High Mg^{2+} Concentrations

Recent studies have demonstrated that Ca^{2+} sparks in frog muscle fibers can still be recorded at high Mg^{2+} concentrations (as high as 7.5 mM), but with diminished amplitude and spatial width (González et al., 2000). Thus, it was of interest to evaluate unitary Ca^{2+} current at such high Mg^{2+} concentrations. Three sample channel records of a single amphibian RyR channel are shown in Fig. 8 A. These records were collected in the presence of 0, 5 (top), or 10 mM Mg^{2+} (added sym-

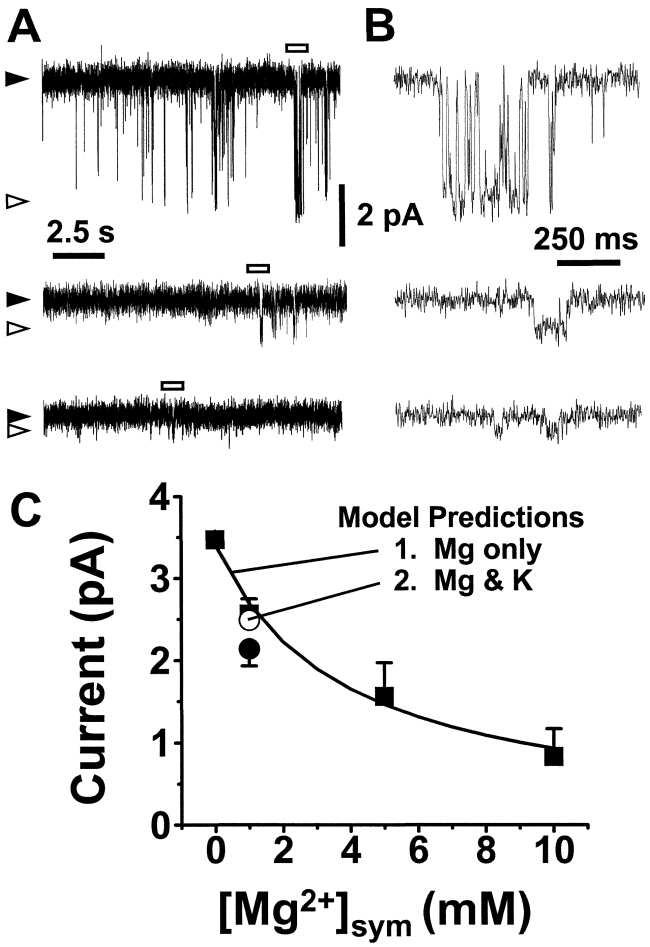

FIGURE 8. Influence of elevated Mg^{2+} on Ca^{2+} current of frog RyR channel. Experiments at 10 mM $[Ca^{2+}]_L$. (A) Current in the presence of symmetric 0, 5 or 10 mM Mg^{2+} (top to bottom). (B) Marked segments of records in A on an expanded time scale. (C) Squares, average currents (± SEM; $n = 3–5$) in different symmetrical Mg^{2+} concentrations. Line, fit with Eq. 1 to predictions of the 4-barrier model. Filled circle, measured current at 1 mM $[Mg^{2+}]$ and 150 mM KCl. Open circle, corresponding prediction of the 4-barrier model.

metrically). The solutions included 10 mM $[Ca^{2+}]_L$ and the usual 10 mM caffeine. An obstacle for the accurate measurement of current attenuation was the clear decrease in Po (expected and observed) at elevated Mg^{2+} concentrations (even in the presence of caffeine). In Fig. 8 A, highly compressed records are shown to illustrate the decrease in Po. In spite of this complication, a few sufficiently long openings were recorded and adequate measurements of current amplitude were made at high Mg^{2+} levels.

Segments from each record (marked by the open bar) are shown expanded in Fig. 8 B. Summary unitary current data are presented in Fig. 8 C (filled squares). The nearly perfect prediction of the 4-barrier model (Tinker et al., 1992) using these same salt conditions is represented by the continuous curve. The filled circle

TABLE I

Unitary Ca^{2+} Current of RyR Channels

Experimental Condition (0 mV; 20 mM $[Ca^{2+}]_L$)	Mammalian RyR2	Amphibian RyR
	pA	*pA*
Control (no competing ions)	4.00 ± 0.08	4.07 ± 0.15
Symmetrical 1 mM Mg^{2+}	3.19 ± 0.11	3.21 ± 0.30
Symmetrical 150 mM K^+	2.64 ± 0.26	2.78 ± 0.21
Symmetrical 1 mM Mg^{2+} + 150 mM K^+	2.20 ± 0.10	2.42 ± 0.20

represents the measured average current in the combined presence of 1 mM Mg^{2+} and 150 mM K^+. The corresponding model prediction (in the combined presence of Mg^{2+} and K^+) is represented by the open circle. In summary, 10 mM symmetrical Mg^{2+} reduced the unitary current carried by 10 mM Ca^{2+} to ~40%.

DISCUSSION

Single RyR channel studies require that the channel be removed from the cell and reconstituted into an artificial membrane system. Consequently, many factors (known or unknown) that affect RyR channel operation will be absent. To maximize the signal-to-noise ratio and minimize the number of variables, most single RyR channel studies have been conducted in relatively simple experimental conditions, typically using a monovalent cation as charge carrier. In cases where Ca^{2+} is the carrier, very large $[Ca^{2+}]_L$s are used and the current is enhanced by the absence of other permeant ions. The present studies were designed to more closely approach the salt conditions that exist in the cell. These include a substantially smaller Ca^{2+} gradient (down to 1 mM $[Ca^{2+}]_L$) and the presence of Mg^{2+} and K^+.

The unitary Ca^{2+} current carried by a RyR channel in the presence of a large $[Ca^{2+}]_L$ without competing permeant ions is well documented. Smith et al. (1988) reported 4.2 pA with 54 mM $[Ca^{2+}]_L$ for rabbit skeletal channels. Tinker and Williams (1992) measured 5.5 pA with 210 mM $[Ca^{2+}]_L$ for sheep cardiac channels. Here, unit Ca^{2+} current was measured both in the absence and presence of other permeant ions. The unit Ca^{2+} currents carried by the mammalian cardiac and amphibian skeletal RyR channels (at 0 mV) with 20 mM $[Ca^{2+}]_L$ were not statistically different ($P > 0.20$, see Table I). The results confirm that physiologic concentrations of K^+ and Mg^{2+} attenuate the unit Ca^{2+} current through both types of RyR channels tested. This head-to-head comparison under identical recording conditions also confirms the similar permeation properties of these RyR channels. We preliminarily reported a two-fold difference in the unitary current carried by the frog and mammalian channels at 150 mM K, 1 mM Mg, and 1 mM lumenal Ca (Kettlun et al., 2000). The

TABLE II

Ca^{2+} Current in Near-physiological Salt Mixtures

	Mammalian RyR2	Amphibian RyR
	pA	*pA*
0.5 mM $[Ca^{2+}]_L$	0.27	0.26
0.75 mM $[Ca^{2+}]_L$	0.39	0.37
1.0 mM $[Ca^{2+}]_L$	0.49	0.48
1.25 mM $[Ca^{2+}]_L$	0.59	0.58

Values taken from single hyperbolic curve fits presented in Fig. 7 D. All experiments were at 0 mV, with symmetrical 1 mM Mg^{2+} and 150 mM K^+.

present results, obtained from more measurements, must supersede the previous report.

Unitary Ca^{2+} Current Measurements

The free Ca^{2+} concentration inside the SR is thought to be near 1 mM in mammalian cardiac muscle (Shannon and Bers, 1997) and amphibian skeletal muscle (Volpe and Simon, 1991). Given the difficulties to directly measure current at such concentrations of the carrier, different theories have been used to predict the Ca^{2+} current through the RyR channel under those conditions. Tinker et al. (1992) used an Eyring-rate permeation model and unitary currents measured at higher than physiological $[Ca^{2+}]_L$ (210 mM Ca^{2+}) to predict that the mammalian RyR2 channel should carry a Ca^{2+} current of ~1.4 pA. Mejía-Alvarez et al. (1999) directly measured Ca^{2+} currents carried by RyR2 channels at a very low $[Ca^{2+}]_L$ in the presence of a competing monovalent cation (symmetrical 150 mM Cs^+, absence of Mg^{2+} and with no transmembrane potential) and reported a unit Ca^{2+} current of 0.35 pA. We have extended these measurements here to include the amphibian RyR channel, and used caffeine to prolong open dwell times. The measurement conditions for the first time included a low $[Ca^{2+}]_L$ in the simultaneous presence of Mg^{2+} and K^+.

As shown in Fig. 7 and Table II, the current in the presence of 1 mM Mg^{2+} and 150 mM K^+ with 1 mM $[Ca^{2+}]_L$ as charge carrier was 0.48 pA for the amphibian channel. The unitary current of the mammalian cardiac channel was similar (0.49 pA). The value reported by Mejía-Alvarez et al. (1999) was ~30% smaller. The most important reason that led to the greater current in the present experiments was probably the stabilization of the open state by caffeine.

Unitary Ca^{2+} Current Predictions

To facilitate extrapolation to conditions that make measurement difficult, the present results were compared with model predictions. To stress these limited, nonmechanistic purposes, two permeation models with different physico-chemical underpinnings were used. One was the discrete state (4-barrier Eyring transition state) model of Tinker et al. (1992). Eyring's transition state theory does not apply to the physics of ion permeation (e.g., Andersen, 1999), in spite of which the model of Tinker et al. (1992) has become a standard descriptive tool in the work with ryanodine receptors. The unitary currents predicted with this model (at 1 mM Ca^{2+}, Fig. 7 D) were ~0.25 pA larger than those measured, but reproduced very well the changes with $[Ca^{2+}]_L$. Predicted Ca^{2+} currents at high Mg^{2+} concentrations (in the absence of KCl) were also compared with our measurements. The model currents in these simpler salt conditions at a higher $[Ca^{2+}]_L$ (10 mM) were nearly identical to the measurements (Fig. 8). The good agreement between the discrete kinetic model predictions and our experiments supports the use of the model as a tool to estimate currents in vivo, in not easily reproducible conditions (for example, when concentrations are varying).

The flow of monovalent cations through RyR2 has also been modeled with an extension of the Poisson-Nernst-Planck or PNP model of electrodiffusion (Chen et al., 1999). Dr. Duan Chen kindly performed calculations with a version of the model modified to include divalents (Chenet al., 2003) using parameter values given in MATERIALS AND METHODS, and found that he could fit well our I versus $[Ca^{2+}]$ data in the presence of K^+ and Mg^{2+}.

In summary, both models proved valuable for prediction and parametrization of RyR channel currents. Either one could be applied, for instance, to predict currents at lower $[Ca^{2+}]_{SR}$ than used in the present measurements.

In the original description of the Ca^{2+} spark in mammalian cardiac muscle (Cheng et al., 1993), the possibility was put forward that these events may be generated by a single RyR channel. This suggestion assumed that the RyR channel had a unitary current of 3 pA (Rousseau and Meissner, 1989) and that the SR Ca^{2+} flux underlying the spark was 4 pA (Cheng et al., 1993). More recently, Soeller and Cannell (2002) concluded that the SR Ca^{2+} flux underlying the spark was 7–12 pA. Here, we show that the unitary current is probably near 0.5 pA with 1 mM $[Ca^{2+}]_L$ present. 8–32 RyR channels with this current would have to open in concert to generate a spark. This is in reasonable agreement with noise analysis suggesting that ~18 RyR channels may be involved in the generation of the spark of cardiac muscle (Bridge et al., 1999).

Other studies in cardiac myocytes, Wang et al. (2003) observed a quantal substructure in sparks, which combined with an internal calibration procedure (based on the observation of sparklets, associated with plasmalemmal L-type channel openings) led to an estimate of 1.2 pA per channel. Another estimate, this time for skeletal

muscle, came from simulations that seek to reproduce long-lasting fluorescence events of low intensity, observed in intact frog skeletal muscle (González et al., 2000). Simulations of these events required a point source (presumably a single channel) of 0.4 pA.

These estimates (0.4–1.2 pA per channel) are relatively close given the differences in approach and conditions, and allow one to evaluate numbers of channels, within a factor of 3, when the collective current intensity is known.

Ca^{2+} sparks are commonly studied in amphibian skeletal muscle (Ríos and Brum, 2002; Schneider and Ward, 2002). In one study, elevated cytosolic Mg^{2+} concentrations (7 mM) greatly reduced the amplitude and spatial width of Ca^{2+} sparks elicited by depolarization in voltage-clamped frog skeletal muscle (González et al., 2000). One possible mechanism of this effect is that the added Mg^{2+} attenuates the unitary Ca^{2+} current, reducing spark width and amplitude, but not its rise time. To test this possibility, studies were performed here at a comparably high Mg^{2+} concentration (Fig. 8). The attenuation of unitary Ca^{2+} current was substantial (~2.5-fold less than in 1 mM Mg^{2+}). Thus, the reduction in Ca^{2+} spark amplitude observed at elevated cytosolic Mg^{2+} levels (González et al., 2000) may in part be due to an attenuation of unitary current. However, these very high Mg^{2+} levels also substantially reduce RyR channel open probability (see Fig. 8). Therefore, the reduced spark amplitude at elevated cytosolic Mg^{2+} levels must reflect a reduction in unitary Ca^{2+} current compounded by a reduction in the number of channels simultaneously open.

We are grateful to Andrew Tinker (University College, London) and Alan L. Williams (Imperial College, London) for generously supplying a program that implements the 4-barrier permeation model. We also thank Le Xu and Gerhard Meissner (University of North Carolina at Chapel Hill) for help in implementation of the barrier model and discussions on the PNP model. We are indebted to Duan P. Chen (Rush University, Chicago) for fitting our data to an updated version of the PNP model. We are also grateful to D.M. Bers (Loyola University Chicago) for many discussions and suggestions.

This work was supported by National Institutes of Health grants HL57832 and HL64210 to M. Fill, and RA32808 to E. Rios. A. Gonzalez was the recipient of a Senior Fellowship of the American Heart Association of Metropolitan Chicago.

Olaf S. Andersen served as editor.

Submitted: 7 April 2003
Accepted: 18 April 2003

REFERENCES

Airey, J.A., M.M. Grinsell, L.R. Jones, J.L. Sutko, and D. Witcher. 1993. Three ryanodine receptor isoforms exist in avian striated muscles. *Biochemistry.* 32:5739–5745.

Andersen, O.S. 1999. Graphic representation of the results of kinetic analyses. *J. Gen. Physiol.* 114:589–590.

Best, P.M., and C.W. Abramcheck. 1985. Potassium efflux from single skinned skeletal muscle fibers. *Biophys. J.* 48:907–913.

Bridge, J.H., P.R. Ershler, and M.B. Cannell. 1999. Properties of Ca^{2+} sparks evoked by action potentials in mouse ventricular myocytes. *J. Physiol.* 518:469–478.

Chen, D.P., L. Xu, A. Tripathy, G. Meissner, and R.S. Eisenberg. 1999. Selectivity and permeation in calcium release channel of cardiac muscle: alkali metal ions. *Biophys. J.* 76:1346–1366.

Chen, D.P., L. Xu, R.S. Eisenberg, and G. Meissner. 2003. Calcium ion permeation through the calcium release channel (ryanodine receptor) of cardiac muscle. *J. Chem. Physiol.* In press.

Chen, W., C. Steenberg, L.A. Levy, J. Vance, R.E. London, and E. Murphy. 1996. Measurements of free Ca^{2+} on sarcoplasmic reticulum in perfuse rabbit heart loaded with 1,2-bis (2-amino-5,6-difluorophenoxy)ethane-N,N,N′,N′-tetraacetic acid by 19F NMR. *J. Biol. Chem.* 271:7398–7403.

Cheng, H., W.J. Lederer, and M.B. Cannell. 1993. Calcium sparks: elementary events underlying excitation-contraction coupling in heart muscle. *Science.* 262:740–744.

Conklin, M.W., P. Powers, R.G. Gregg, and R. Coronado. 1999. Ca^{2+} sparks in embryonic mouse skeletal muscle selectively deficient in dihydropyridine receptor alpha1S or beta1a subunits. *Biophys. J.* 76:657–669.

Coronado, R., J. Morrissette, M. Sukhareva, and D.M. Vaughan. 1994. Structure and function of ryanodine receptors. *Am. J. Physiol.* 266:C1485–C1504.

Felder, E., and C. Franzini-Armstrong. 2002. Type 3 ryanodine receptors of skeletal muscle are segregated in a parajunctional position. *Proc. Natl. Acad. Sci. USA.* 99:1695–1700.

Fill, M., and R. Coronado. 1988. Ryanodine receptor channel of sarcoplasmic reticulum. *Trends Neurosci.* 11:453–457.

Fill, M., R. Coronado, J.R. Mickelson, J. Vilven, J.J. Ma, B.A. Jacobson, and C.F. Louis. 1990. Abnormal ryanodine receptor channels in malignant hyperthermia. *Biophys. J.* 57:471–475.

Froemming, G.R., B.E. Murray, S. Harmon, D. Pette, and K. Ohlendieck. 2000. Comparative analysis of the isoform expression pattern of Ca^{2+}-regulatory membrane proteins in fast-twitch, slow-twitch, cardiac, neonatal and chronic low-frequency stimulated muscle fibers. *Biochim. Biophys. Acta.* 1466:151–168.

Gilbert, J.R., and G. Meissner. 1983. Na^+, K^+, H^+ and Cl^- permeability properties of rabbit skeletal muscle sarcolemmal vesicles. *Arch. Biochem. Biophys.* 223:9–23.

González, A., W.G. Kirsch, N. Shirokova, G. Pizarro, M.D. Stern, and E. Ríos. 2000. The spark and its ember: separately gated local components of Ca^{2+} release in skeletal muscle. *J. Gen. Physiol.* 115:139–158.

Inesi, G. 1994. Teaching active transport at the turn of the 21st century. *Biophys. J.* 66:554–560.

Hasselbach, W., and H. Oetliker. 1983. Energetics and electrogenicity of the sarcoplasmic reticulum calcium pump. *Annu. Rev. Physiol.* 45:325–339.

Kettlun, C., A. González, E. Ríos, and M. Fill. 2000. Ryanodine receptor unitary Ca^{2+} current amplitude in frog skeletal muscle. *Biophys. J.* 78:437a.

Kirsch, W.G., D. Uttenweiler, and R.H. Fink. 2001. Spark- and ember-like elementary Ca^{2+} release events in skinned fibers of adult mammalian skeletal muscle. *J. Physiol.* 537:379–389.

Klein, M.G., H. Cheng, L.F. Santana, Y.H. Jiang, W.J. Lederer, and M.F. Schneider. 1996. Two mechanisms of quantized calcium release in skeletal muscle. *Nature.* 379:455–458,

Lai, F.A., Q.Y. Liu, I. Xu, A. El-Hashem, N.R. Kramarcy, R. Sealock, and G. Meissner. 1992. Amphibian ryanodine receptor isoforms are relates to those of mammalian skeletal or cardiac muscle. *Am. J. Physiol.* 263:C365–C372.

Lamb, G.D. 2000. Excitation-contraction coupling in skeletal muscle: comparisons with cardiac muscle. *Clin. Exp. Pharmacol. Phys-*

iol. 27:216–224.

Lamb, G.D. 2002. Voltage-sensor control of Ca^{2+} release in skeletal muscle: insights from skinned fibers. *Front. Biosci.* 7:d834–d842.

Lindsay, A.R., S.D. Manning, and A.J. Williams. 1991. Monovalent cation conductance in the ryanodine receptor-channel of sheep cardiac muscle sarcoplasmic reticulum. *J. Physiol.* 439:463–480.

McPherson, P.S., and K.P. Campbell. 1993. The ryanodine receptor/Ca^{2+} release channel. *J. Biol. Chem.* 268:13765–13768.

Meissner, G., E. Ríos, A. Tripathy, and D.A. Pasek. 1997. Regulation of skeletal muscle Ca^{2+} released channel (Ryanodine Receptor) by Ca^{2+} and monovalent cations and anions. *J. Biol. Chem.* 272: 1628–1638.

Mejía-Alvarez, R., C. Kettlun, E. Ríos, M. Stern, and M. Fill. 1999. Unitary Ca^{2+} current through cardiac ryanodine receptor channels under quasi-physiological ionic conditions. *J. Gen. Physiol.* 113:177–186.

Murayama, T., O. Toshiharu, E. Katayama, H. Oyadama, K. Oguchi, M. Kobayashi, K. Otsuka, and Y. Ogawa. 1999. Further characterization of the type 3 ryanodine receptor (RyR3) purified from rabbit diaphragm. *J. Biol. Chem.* 274:17297–17308.

Ogawa, Y. 1994. Role of ryanodine receptors. *Crit. Rev. Biochem. Mol. Biol.* 29:229–274.

Oyamada, H., T. Murayama, T. Takagi, M. Iino, N. Iwabe, T. Miyata, Y. Ogawa, and M. Endo. 1994. Primary structure and distribution of ryanodine-binding protein isoforms of the bullfrog skeletal muscle. *J. Biol. Chem.* 269:17206–17214.

Ríos, E., and G. Brum. 2002. Ca^{2+} release flux underlying Ca^{2+} transients and Ca^{2+} sparks in skeletal muscle. *Front. Biosci.* 7:d1195–d1211.

Ríos, E., and G. Pizarro. 1991. Voltage sensor of excitation contraction coupling in skeletal muscle. *Physiol. Rev.* 71:849–908.

Rosner, B. 1982. Fundamental of Biostatistics. Duxbury Press. Boston, MA.

Rousseau, E., and G. Meissner. 1989. Single cardiac sarcoplasmic reticulum Ca^{2+}-release channel: activation by caffeine. *Am. J. Physiol.* 256:H328–H333.

Schneider, M.F., and C.W. Ward. 2002. Initiation and termination of calcium sparks in skeletal muscle. *Front. Biosci.* 7:d1212–d1222.

Shannon, T.R., and D.M. Bers. 1997. Assessment of intra-SR free [Ca^{2+}] and buffering in rat heart. *Biophys. J.* 73:1524–1531.

Smith, J.S., R. Coronado, and G. Meissner. 1985. Sarcoplasmic reticulum contains adenine nucleotide-activated calcium channels. *Nature.* 316:446–449.

Smith, J.S., T. Imagawa, J. Ma, M. Fill, K.P. Campbell, and R. Coronado. 1988. Purified ryanodine receptor from rabbit skeletal muscle is the calcium-release channel of sarcoplasmic reticulum. *J. Gen. Physiol.* 92:1–26.

Soeller, C., and M.B. Cannell. 2002. Estimation of the sarcoplasmic reticulum Ca^{2+} release flux underlying Ca^{2+} sparks. *Biophys. J.* 82: 2396–2414.

Somlyo, A.V., H.G. González-Serratos, H. Shuman, G. McClellan, and A.P. Somlyo. 1981. Calcium release and ionic changes in the sarcoplasmic reticulum of tetanized muscle: an electron-probe study. *J. Cell Biol.* 90:577–594.

Sutko, J.L., J.A. Airey, K. Murakami, M. Takeda, C.F. Beck, T.J. Deerinck, and M.H. Ellisman. 1991. Foot protein isoforms are expressed at different times during embryonic chicken skeletal muscle development. *J. Cell Biol.* 113:793–803.

Sutko, J.L., and J.A. Airey. 1996. Ryanodine receptor Ca^{2+} release channels: does diversity in form equal diversity in function? *Physiol. Rev.* 76:1027–1071.

Tang, J.M., J. Wang, and R.S. Eisenberg. 1989. K^{+}-selective channel from sarcoplasmic reticulum of split lobster muscle fibers. *J. Gen. Physiol.* 94:261–278.

Tarroni, P., D. Rossi, A. Conti, and V. Sorrentino. 1997. Expression of the ryanodine receptor type 3 calcium release channel during development and differentiation of mammalian skeletal muscle cells. *J. Biol. Chem.* 272:19808–19813.

Tate, C.A., R.J. Bick, A. Chu, W.B. Van Winkle, and M.L. Entman. 1985. Nucleotide specificity of cardiac sarcoplasmic reticulum. GTP-induced calcium accumulation and GTPase activity. *J. Biol. Chem.* 260:9618–9623.

Tinker, A., and A.J. Williams. 1992. Divalent cation conduction in the ryanodine receptor channel of sheep cardiac muscle sarcoplasmic reticulum. *J. Gen. Physiol.* 100:479–493.

Tinker, A., A.R.G. Lindsay, and A.J. Williams. 1992. A model for ionic conduction in the ryanodine receptor channel of sheep cardiac muscle sarcoplasmic reticulum. *J. Gen. Physiol.* 100:495–517.

Tsugorka, A., E. Ríos, and L.A. Blatter. 1995. Imaging elementary events of calcium release in skeletal muscle cells. *Science.* 269: 1723–1726.

Volpe, P., and B.J. Simon. 1991. The bulk of Ca^{2+} released to the myoplasm is free in the sarcoplasmic reticulum and does not unbind from calsequestrin. *FEBS Lett.* 278:274–278.

Wang, S.Q., L.S. Song, E.G. Lakatta, and H. Cheng. 2001. Ca^{2+} signaling between single L-type Ca^{2+} channels and ryanodine receptors in heart cells. *Nature.* 410:592–596.

Wang, S.Q., M.D. Stern, E. Ríos, and H. Cheng. 2003. The quantal nature of Ca^{2+} sparks reveals nanoscopic interaction between ryanodine receptors in vivo. *Biophys. J.* 84:385a.

Williams, A.J., D.J. West, and R. Sitsapesan. 2001. Light at the end of the Ca^{2+}-released channel tunnel: structures and mechanisms involved in ionic translocation in ryanodine receptor channels. *Q. Rev. Biophys.* 34:61–104.

Zhou, J., G. Brum, A. Gonzalez, B.S. Launikonis, M.D. Stern, and E. Rios. 2003. Ca^{2+} Sparks and embers of mammalian muscle. Properties of the sources. *J. Gen. Physiol.* 122:95–114.